Neurosci. Bull. October, 2019, 35(5):853–866
https://doi.org/10.1007/s12264-019-00375-8

www.neurosci.cn
www.springer.com/12264

ORIGINAL ARTICLE

Myelin Oligodendrocyte Glycoprotein-IgG Contributes to Oligodendrocytopathy in the Presence of Complement, Distinct from Astrocytopathy Induced by AQP4-IgG

Ling Fang[1] · Xinmei Kang[1] · Zhen Wang[2,3] · Shisi Wang[1] · Jingqi Wang[1] · Yifan Zhou[1] · Chen Chen[1] · Xiaobo Sun[1] · Yaping Yan[3] · Allan G. Kermode[1,4] · Lisheng Peng[1] · Wei Qiu[1]

Received: 12 October 2018 / Accepted: 18 January 2019 / Published online: 30 April 2019

Abstract Immunoglobulin G against myelin oligodendrocyte glycoprotein (MOG-IgG) is detectable in neuromyelitis optica spectrum disorder (NMOSD) without aquaporin-4 IgG (AQP4-IgG), but its pathogenicity remains unclear. In this study, we explored the pathogenic mechanisms of MOG-IgG *in vitro* and *in vivo* and compared them with those of AQP4-IgG. MOG-IgG-positive serum induced complement activation and cell death in human embryonic kidney (HEK)-293T cells transfected with human MOG. In C57BL/6 mice and Sprague-Dawley rats, MOG-IgG only caused lesions in the presence of complement. Interestingly, AQP4-IgG induced astroglial damage, while MOG-IgG mainly caused myelin loss. MOG-IgG also induced astrocyte damage in mouse brains in the presence of complement. Importantly, we also observed ultrastructural changes induced by MOG-IgG and AQP4-IgG. These findings suggest that MOG-IgG directly mediates cell death by activating complement *in vitro* and producing NMOSD-like lesions *in vivo*. AQP4-IgG directly targets astrocytes, while MOG-IgG mainly damages oligodendrocytes.

Keywords Neuromyelitis optica spectrum disorder · Aquaporin-4 immunoglobulin G · Myelin oligodendrocyte glycoprotein immunoglobulin G · Complement-dependent cytotoxicity · Transmission electron microscopy

Introduction

Neuromyelitis optica spectrum disorder (NMOSD) was considered to be a locally restricted form of multiple sclerosis until Lennon [1] discovered aquaporin-4 immunoglobulin G (AQP4-IgG) in 2004. It is generally accepted that AQP4-IgG crosses the damaged blood-brain barrier and targets the water channel AQP4 expressed on the surface of astrocytic end-feet, inducing complement-mediated necrosis, secondary demyelination, inflammation, and neuronal death [2]. According to the 2015 international consensus diagnostic criteria [3], NMOSD with AQP4-IgG is an autoimmune astrocytopathy of the central nervous system, while NMOSD without AQP4-IgG includes a subgroup of patients with myelin oligodendrocyte glycoprotein (MOG)-IgG, suggesting a different underlying pathogenesis.

MOG-IgG is present in 20%–42% of AQP4-IgG-seronegative NMOSD patients [4, 5]; it is also detectable using cell-based assays in individuals with acute disseminated encephalomyelitis, optic neuritis, and acute transverse myelitis [6–9]. Although it is generally believed

Ling Fang, Xinmei Kang, and Zhen Wang contributed equally to this work.

✉ Lisheng Peng
penglsh5@mail.sysu.edu.cn

✉ Wei Qiu
qiuwei120@vip.163.com

[1] Department of Neurology, The Third Affiliated Hospital of Sun Yat-sen University, Guangzhou 510000, China

[2] Department of Neurology, Xuanwu Hospital, Capital Medical University, Beijing 100053, China

[3] Key Laboratory of the Ministry of Education for Medicinal Resources and Natural Pharmaceutical Chemistry, National Engineering Laboratory for Resource Development of Endangered Crude Drugs in Northwest China, College of Life Sciences, Shaanxi Normal University, Xi'an 710119, China

[4] Department of Neurology, Centre for Neuromuscular and Neurological Disorders, Queen Elizabeth II Medical Centre, Sir Charles Gairdner Hospital, University of Western Australia, Perth, WA 6009, Australia

that MOG-IgG is only present in AQP4-IgG seronegative patients, NMOSD patients carrying both AQP4-IgG and MOG-IgG have also been reported [10]. Pathogenic MOG-IgG appears to recognize only the native conformational state of MOG [11–15]. There are clinical differences between NMOSD patients positive for MOG-IgG and AQP4-IgG, the former are younger, more often male, are more likely to have involvement of the conus and deep gray matter structures on imaging, and have more favorable outcomes [4, 16–18]. Meanwhile, recent studies have reported that MOG-IgG-positive optic neuritis and/or myelitis may be more severe than previously thought, leaving residual neurological deficits [9, 19]. Furthermore, patients with MOG-IgG-associated disease are more likely to have seizures and an encephalitis-like presentation than patients with AQP4-IgG-associated disease [20]. In cohort studies, we screened MOG-IgG-seropositive patients using an in-house live-cell-based assay and concluded that the onset phenotype may influence the long-term presentation and MOG-IgG status as well as the outcome [21], and pediatric-onset and adult-onset patients with MOG-IgG exhibit distinct features [22].

The pathogenicity of mouse MOG-IgG has been well studied [23–25]. However, because of the rarity of patients whose sera cross-react with mouse MOG (as only a subset of human MOG antibodies reacts with mouse or rat MOG [8, 26–29]), acquiring human MOG-IgG samples suitable for animal experiments has been a challenge. Moreover, standard MOG-IgG assays are not yet widely available [30], so only a few studies have investigated human MOG-IgG *in vivo* [28, 29, 31–33]. One major unresolved issue is whether the complement system contributes to the formation of MOG-IgG-mediated lesions. Therefore, we aimed to explore the pathogenic mechanisms of MOG-IgG *in vitro* and *in vivo* and to compare them with those of AQP4-IgG.

Materials and Methods

Materials

Animals

Eight- to twelve-week-old female C57BL/6 mice and female Sprague-Dawley rats were purchased from Guangdong Medical Laboratory Animal Center, maintained in air-filtered cages, and fed normal rodent chow. All the experiments were performed in accordance with the national institutes of health guide for the care and use of animals with approval from the institutional Animal Care Committee and the Ethics Committee of the Third Affiliated Hospital of Sun Yat-sen University.

Screening the Reactivity of Serum to Human, Mouse, and Rat MOG

MOG-IgG serum was screened following our previously described methodology [21, 22]. Human embryonic kidney 293T (HEK-293T) cells stably transfected with plasmids encoding full-length human MOG and green fluorescent protein (GFP) were incubated with patient sera [diluted 1:10 in Dulbecco's modified Eagle's medium (DMEM) (Gibco, 11965-092, Grand Island, Nebraska, USA)] for 40 min, then with Alexa Fluor® 546-labeled goat anti-human IgG (H+L, Life Technologies, Invitrogen, A-21089, Tallahassee, Florida, USA) for 30 min at room temperature. Reactivity was assessed using a fluorescence microscope (Leica, DM 4000 B, Wetzlar, Germany). Transfected cells were stained fluorescent green, and red fluorescence appeared when binding of human MOG-IgG occurred.

HEK-293T cells stably transfected with plasmids encoding mouse or rat MOG and GFP were incubated with sera containing high titers of human MOG-IgG to determine the degrees of cross-reactivity.

IgG and Complement Preparation

Total IgG was purified from the serum or plasma of seropositive patients (one NMOSD patient was AQP4-IgG seropositive, and nine were MOG-IgG seropositive) (Table 1) and healthy volunteers using protein A beads (GE Healthcare, 71149800-EG, Boston, Massachusetts, USA). The beads were eluted with 0.1 mol/L glycine-HCl (pH 2.5), then the eluent was concentrated using Amicon Ultra-15 centrifugal filter units (100 kD, Millipore, Billerica, MA). The purified IgG samples were named IgG_{AQP4} (20 mg/mL), IgG_{CON} (20 mg/mL), and IgG_{MOG} [mixed anti-mouse-MOG IgG from five patients (patients 1 to 5, 4.7 mg/mL) and mixed anti-rat-MOG IgG from four patients (patients 6 to 9, 3.6 mg/mL)]. Details of the IgG samples from the 9 MOG-IgG positive patients are listed in Table 1. Human complement (hC) from Innovative Research (IPLA-CSER, Innovative Research, Novi, MI) was stored at − 80 °C. The protocol was approved by the Ethics Committee of the Third Affiliated Hospital of Sun Yat-sen University (Guangzhou, China). Written informed consent was provided by all patients.

Complement Activation and Cytotoxicity Assays In Vitro

HEK-293T cells stably transfected with plasmids encoding full-length human MOG and GFP were incubated at 37 °C in 300 μL DMEM (Gibco, 11965-092) containing 20% (v/v) serum from MOG-IgG seropositive patients ($Serum_{MOG}$) or healthy volunteers ($Serum_{Control}$) with or without hC. IgG samples had been heated at 56 °C for 30 min in

Table 1 Details of the IgG samples from the 9 MOG-IgG and 1 AQP4-IgG positive patients used in this study.

Patient #	Sex	Age (years)	Cell-based assay			Complement activation	Cytotoxicity assays	Final diagnosis
			Antibody titer	rMOG	mMOG			
1	F	19	1:100	+	+	+	+	MS
2	M	10	1:100	−	+	+	+	ADEM
3	M	45	1:100	+	+	+	+	ON
4	F	7	1:100	+	+	+	+	ADEM
5	M	13	1:320	+	+	+	+	ADEM
6	M	8	1:100	+	−	+	+	ADEM
7	F	26	1:320	+	−	+	+	NMOSD
8	M	13	1:640	+	−	+	+	MS
9	F	7	1:1280	+	−	+	+	ADEM
10	F	32	1:320			+	+	NMOSD

Patients 1 to 9 were MOG-IgG positive and Patient 10 was AQP4-IgG positive. MS, multiple sclerosis; ADEM, acute disseminated encephalomyelitis; ON, optic neuritis; NMOSD, neuromyelitis optica spectrum disorder.

advance to destroy serum complement. After 2 h, cells on coverslips were immunostained with an antibody against C5b-9 (1:300, Abcam, ab55811, Cambridge, UK) or with propidium iodide (Sangon Biotech, E607306, Shanghai, China). Dead cells were stained red. A Leica DM 4000 B microscope was used to examine the coverslips. To deplete MOG-IgG, the $Serum_{MOG}$ was adsorbed by incubation with MOG-HEK cells until MOG-IgG became

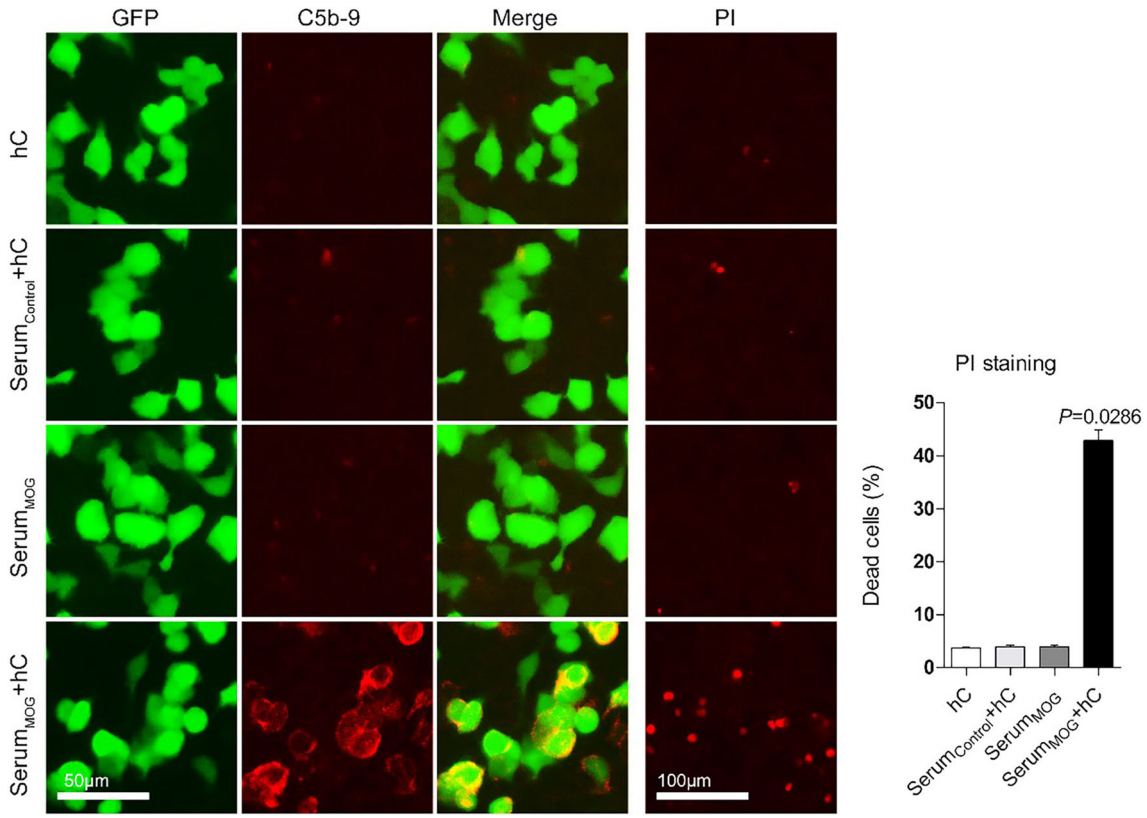

Fig. 1 Human MOG-IgG-positive serum caused death of HEK-293T cells dependent of complement. Left, representative images of MOG-expressing HEK-293T cells incubated with serum from healthy people ($Serum_{Control}$) and MOG-IgG-positive patients ($Serum_{MOG}$) with or without hC (C5b-9), after immunostaining and PI staining. Right, percentages of dead cells (mean ± SEM, $n = 4$, $P = 0.0286$). GFP: co-transfected with MOG, making cells fluorescent green if successfully expressing MOG. PI: dead cells stained red.

undetectable ($Serum_{MOG(AdsMOG\text{-}HEK)}$). $Serum_{MOG}$ adsorbed against non-transfected HEK cells ($Serum_{MOG(AdsHEK)}$) was used as control.

Animal Studies

Intracerebral Injection

Mice were anesthetized by isoflurane inhalation delivered by mask (2% gas in air mixture) and mounted in a stereotaxic frame (RWD Life Science, Shenzhen, China). A burr hole (1 mm diameter) was made 2 mm to the right of bregma using a high-speed drill (RWD Life Science). A 26-gauge needle attached to a 10 μL gas-tight glass syringe was inserted to a depth of 3 mm and either (i) 3 μL total IgG (IgG_{CON}, IgG_{AQP4}, or IgG_{MOG}) in combination with 2 μL hC (at 1 μL/min) or (ii) 5 μL total IgG purified from seropositive patients or healthy volunteers (IgG_{CON}, IgG_{AQP4}, or IgG_{MOG}) alone was infused. After 1 or 5 days, mice were anesthetized with 0.3 mL of 2% sodium pentobarbital and perfused through the left cardiac ventricle with 20 mL phosphate-buffered saline (PBS) followed by 25 mL PBS containing 4% paraformaldehyde.

Procedures for the rat experiments were similar. At a point 2.75 mm to the right of bregma, a 26-gauge needle attached to a 10 μL gas-tight glass syringe was inserted to a depth of 3.75 mm and 10 μL of total IgG purified from patients or healthy individuals (IgG_{CON}, IgG_{AQP4}, or IgG_{MOG}) was infused. Rats were sacrificed 5 days later.

Female C57BL/6 mice were divided into six experimental groups: (i) IgG_{CON} + hC (n = 7), (ii) IgG_{AQP4} + hC (n = 7), (iii) IgG_{MOG} + hC (n = 7), (iv) IgG_{CON} (n = 10),

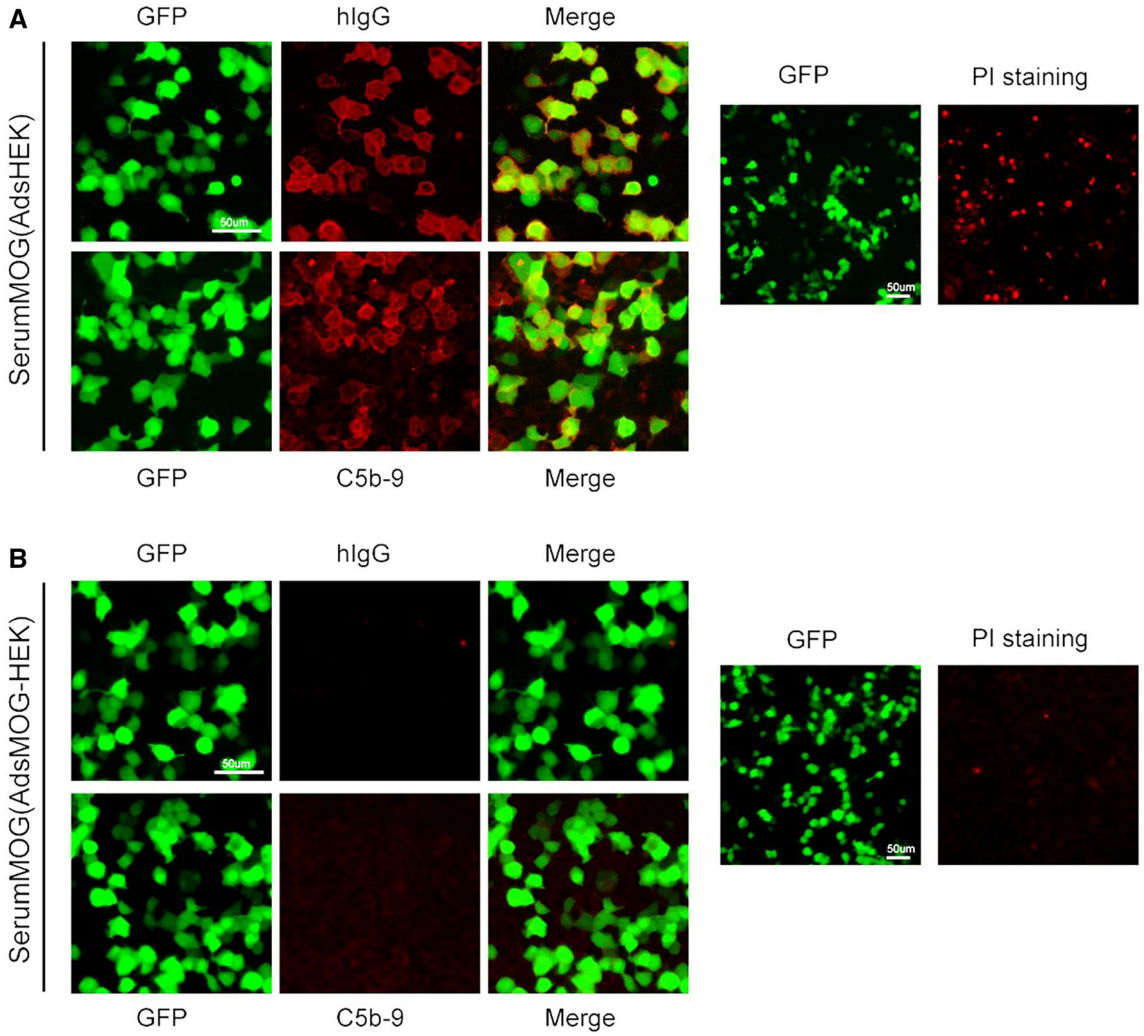

Fig. 2 Serum from which MOG had been adsorbed by incubation with MOG-expressing HEK-293T cells ($Serum_{MOG(AdsMOG\text{-}HEK)}$) did not cause C5b-9 deposition and the death of HEK-293T cells expressing human MOG (**B**), unlike $Serum_{MOG}$ adsorbed against non-transfected HEK-293T cells ($Serum_{MOG(AdsHEK)}$) (**A**). GFP, co-transfected with MOG, making cells fluorescent green if successfully expressing MOG; PI, dead cells stained red.

(v) IgG_{AQP4} (n = 10), and (vi) IgG_{MOG} (n = 10). Female Sprague-Dawley rats were divided into three experimental groups: (i) IgG_{CON} (n = 3), (ii) IgG_{AQP4} (n = 3), and (iii) IgG_{MOG} (n = 3). Investigators were blinded as to whether total IgG from seropositive patients or healthy volunteers was used during the experiments.

Immunofluorescence

Brains were post-fixed for 48 h in 4% paraformaldehyde, then immersed in PBS containing 20%, 25%, and 30% sucrose at 4 °C overnight. Twenty-micron sections through the injection track were cut from frozen brains and incubated in 0.1% Triton-X 100 for 20 min. The sections were blocked with 10% goat serum for 40 min at room temperature, then immunostained overnight at 4 °C with primary antibodies against human IgG (1:500, Life Technologies, Invitrogen Alexa Fluor® 488, A-11013), C5b-9 (1:100, Abcam, ab55811), AQP4 (1:300, Santa Cruz Biotechnology, sc-20812, Dallas, Texas, USA), glial fibrillary acidic protein (GFAP, 1:500, Aves, GFAP7857983, Davis, California, USA), myelin basic protein (MBP, 1:500, Proteintech, 10458-1-AP, Chicago, Illinois, USA), Ly-6G (1:300, BD Biosciences, 562737, San Jose, California, USA), macrophages/microglia [1:300, Santa Cruz Biotechnology, sc-101447, or Iba-1 (1:300, EMD Millipore Corp, ABN67)], or CD3 (1:300, Santa Cruz Biotechnology, sc-101442). Afterwards, the sections were stained with an appropriate species-specific Alexa Fluor-conjugated secondary antibody for 1 h at room temperature. Sections were examined under a Leica DM 4000 B microscope. AQP4, GFAP, and MBP immunonegative areas and macrophage marker immunopositive areas were defined by hand and quantified using ImageJ software (National Institutes of Health, USA, Version 1.51k).

Electron Microscopy

Mice were perfused with ice-cold paraformaldehyde-glutaraldehyde fixative and their brains were cut into 1-mm slices through the injection track. The region of interest (1 mm from the injection point) was post-fixed in 2.5% neutral glutaraldehyde for $>$ 2 h at 4 °C then in 1% osmic acid for 1.5 h–2 h, dehydrated in ethyl alcohol and acetone, embedded in Epon 812, sectioned on an ultramicrotome (Leica, UC-7, 50 nm–70 nm thick), stained with uranyl acetate followed by lead citrate, and then imaged (Tecnai 12 Transmission Electron Microscope).

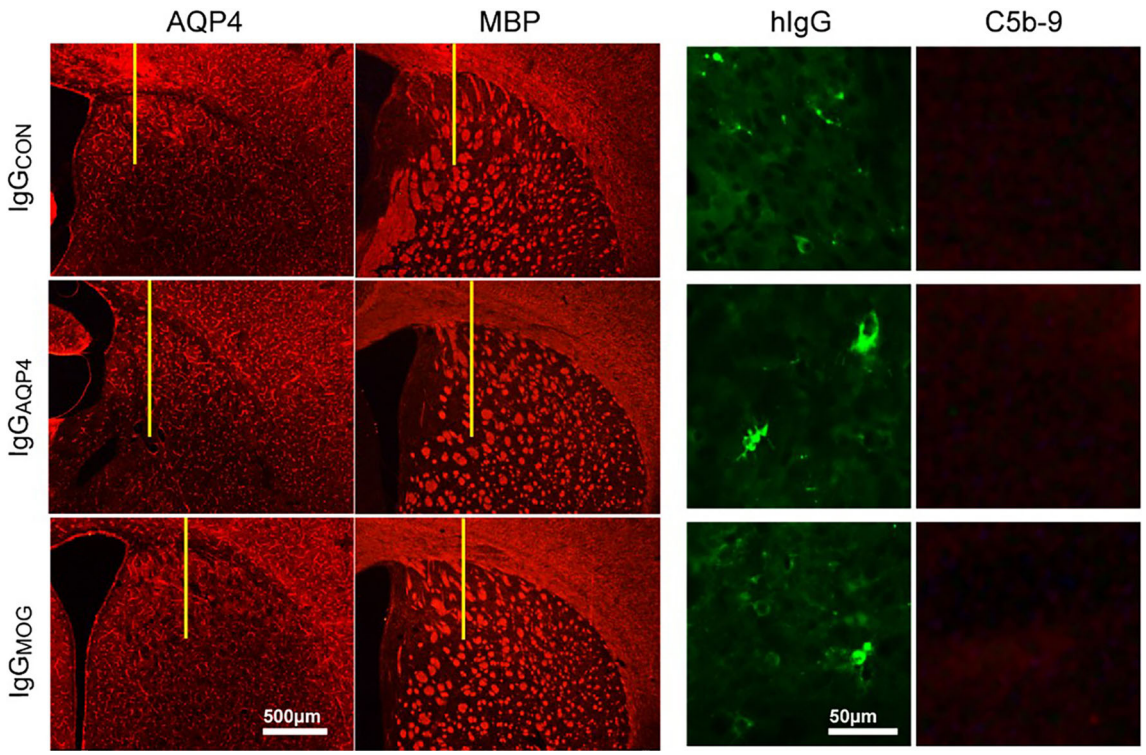

Fig. 3 Neither IgG_{AQP4} nor IgG_{MOG} caused brain damage without complement in C57BL/6 mice. Representative images of sections cut through the injection site in mice 24 h after IgG_{CON}, IgG_{AQP4}, or IgG_{MOG} injection. Human IgG (hIgG) binding was present in all three groups (right), but no deposition of C5b-9 (right) and no loss of AQP4 or MBP were found (left, yellow line, needle track).

Statistics

Data are presented as mean ± SEM, and statistical analysis was performed using GraphPad Prism 5 (GraphPad). We compared data between two groups using Student's *t*-test or the Mann-Whitney *U* test ($\alpha = 0.05$). Comparisons among three groups were made using one-way ANOVA or the Kruskal-Wallis test ($\alpha = 0.05$) followed by the adjusted Mann-Whitney test (corrected $\alpha = 0.05/3$).

Results

Human MOG-IgG-Positive Serum Activated Complement and Caused Cell Death *In Vitro*

We evaluated the pathogenic MOG-IgG-positive sera from 9 patients independently (Table 1). Neither exposure to hC alone nor to hC and healthy control serum caused terminal complement complex C5b-9 deposition and the death of HEK-293T cells expressing human MOG (Fig. 1). C5b-9 deposition and cell death were not observed in HEK-293T cells incubated with serum from MOG-IgG-positive patients alone (Fig. 1), while the sera from all nine MOG-IgG-positive patients led to cell death and C5b-9 deposition in the presence of complement (Table 1, Fig. 1), indicating that human MOG-IgG-positive serum causes the death of HEK-293T cells in a complement-dependent manner.

To further establish that the damage is due to MOG-IgG itself, we repeated the experiment with confirmed MOG-IgG-depleted sera (Fig. 2). $Serum_{MOG}$ was adsorbed by incubation with MOG-expressing HEK293T cells until MOG-IgG became undetectable ($Serum_{MOG(AdsMOG\text{-}HE)}$). This serum did not cause C5b-9 deposition and the death of HEK-293T cells expressing human MOG-(Fig. 2B), unlike $Serum_{MOG}$ adsorbed against non-transfected HEK293T cells ($Serum_{MOG(AdsHEK)}$) (Fig. 2A).

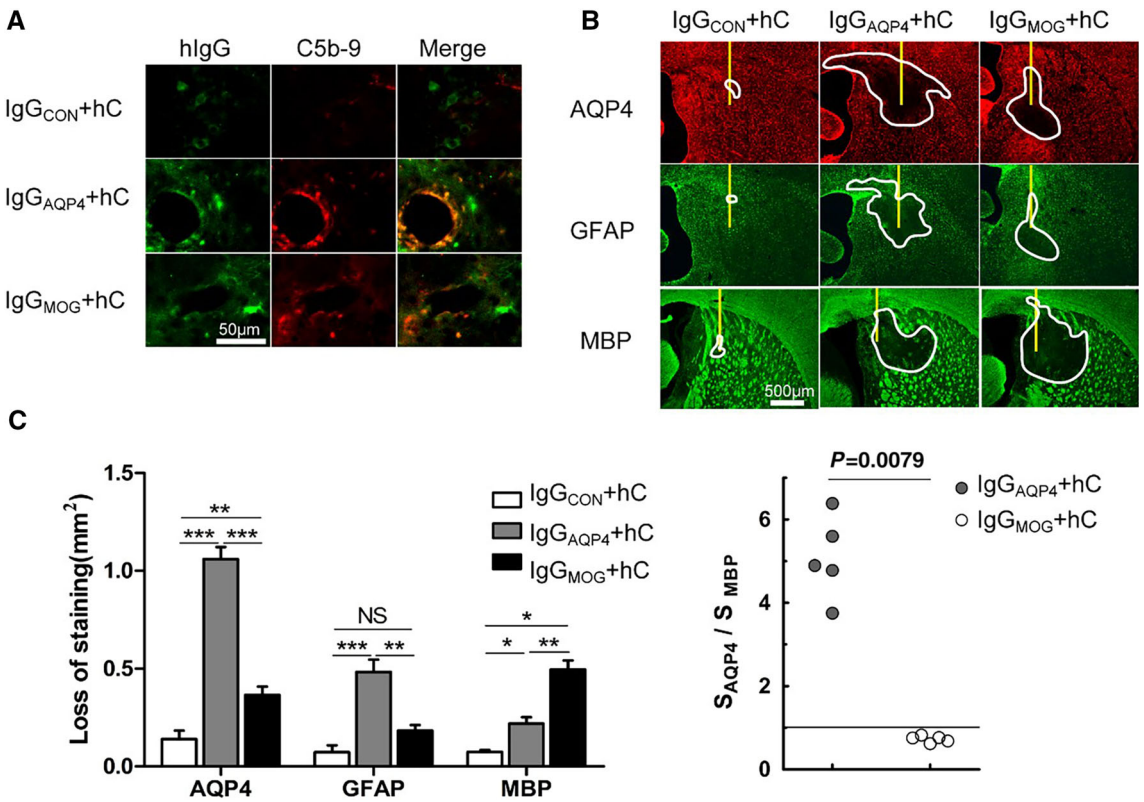

Fig. 4 Both IgG_{AQP4} and IgG_{MOG} damage the mouse brain by complement activation. Mice receiving 3 μl IgG (IgG_{CON}, IgG_{AQP4}, or IgG_{MOG}) plus 2 μl hC were killed at 5 days and coronal sections were cut through the injection site. **A** Representative images showing a human IgG (hIgG)-positive area in all three groups, while only IgG_{AQP4}/IgG_{MOG} plus hC caused C5b-9 deposition. **B** Both IgG_{AQP4} and IgG_{MOG} caused loss of staining for AQP4, GFAP, and MBP dependent on complement activation (yellow line, needle track; white line, lesion border). **C** Left, areas of loss of AQP4, GFAP, and MBP at day 5 (mean ± SEM, $n = 5$, $^{*}P < 0.0167$, $^{**}P < 0.01$, $^{***}P < 0.001$, NS not significant). Right, ratios of AQP4- to MBP-depleted areas (SAQP4/SMBP) in the two groups (mean ± SEM, $n = 5$, $P = 0.0079$).

Neither IgG_{AQP4} nor IgG_{MOG} Caused Parenchymal Damage *In Vivo* in the Absence of Complement

To determine whether the brain parenchyma can be damaged by AQP4-IgG or MOG-IgG itself, we injected total IgG purified from seropositive patients or healthy volunteers into mouse brains in the absence of complement by using the low activity of the classical complement pathway and the presence of complement inhibitor(s) in mouse serum [34]. At 24 h, human IgG binding, but no C5b-9 deposition and no loss of AQP4 or MBP, occurred next to the needle track in all three groups (Fig. 3). Similarly, no loss of AQP4 or MBP was observed at day 5. Therefore, IgG_{AQP4} and IgG_{MOG} do not induce NMOSD-like lesions when injected into the brains of C57BL/6 mice without complement.

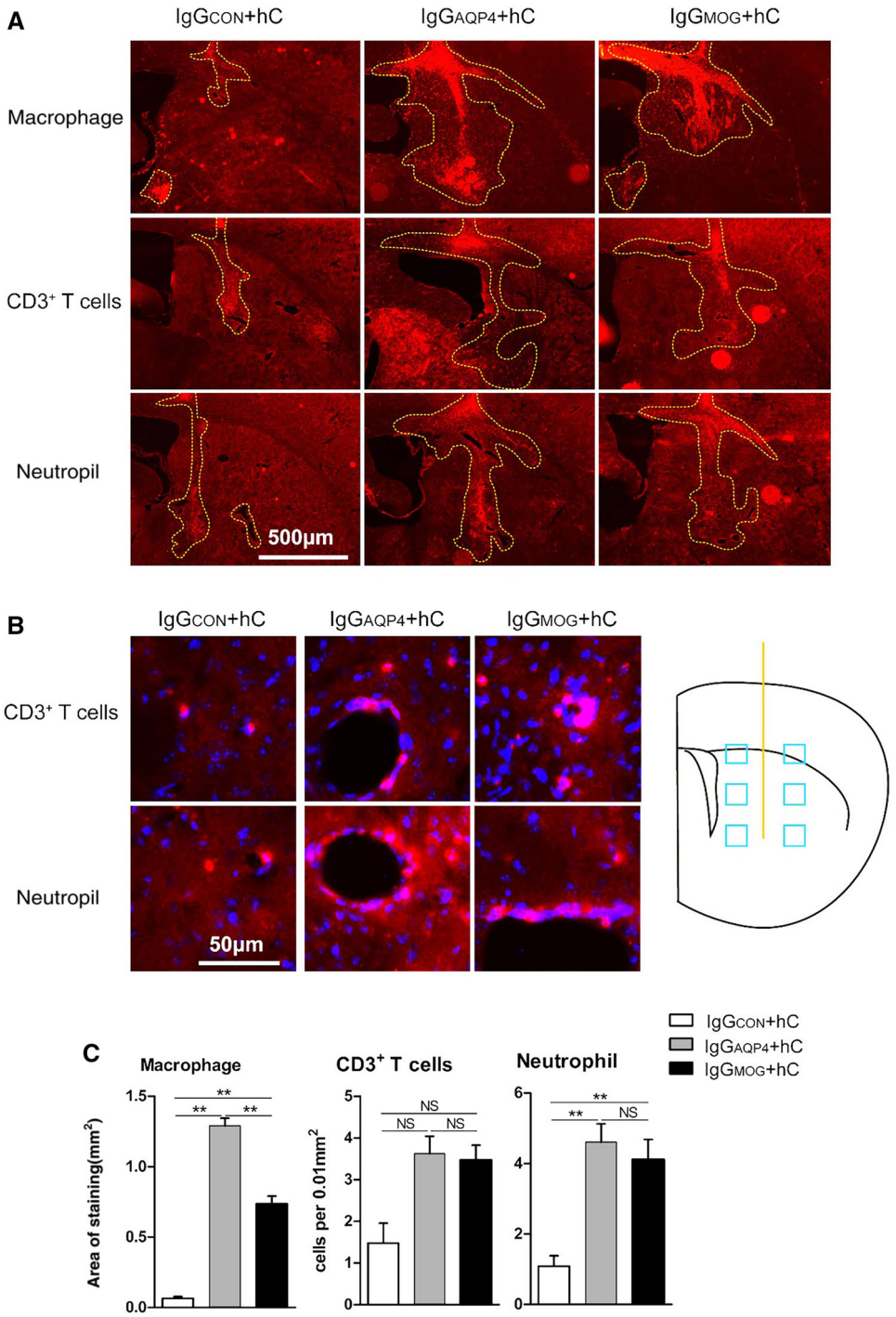

Fig. 5 Both IgG_{AQP4} and IgG_{MOG} caused inflammatory cell infiltration by complement activation. Mice receiving 3 μL of IgG (IgG_{CON}, IgG_{AQP4} or IgG_{MOG}) plus 2 μL hC were killed at 5 days and coronal sections were cut through the injection site. **A** Representative images of immunostaining with macrophage marker (macrophage), Ly-6G (neutrophils), and CD3 ($CD3^+$T cells) (dotted lines, areas with positive inflammatory cells). **B** Left, higher magnification of immunostained neutrophils and $CD3^+$ T cells. Right, schematic showing needle track and areas examined for neutrophils and $CD3^+$ T cells. **C** Macrophage-positive areas and numbers of neutrophils and $CD3^+$T cells at day 5 (mean ± SEM, $n = 5$, $^*P < 0.05/3$, $^{**}P < 0.01$, $^{***}P < 0.001$, NS not significant).

IgG_{MOG} Mainly Targeted Myelin While Igg_{AQP4} Targeted Astrocytes

We injected mouse brains with a mixture of 3 μL IgG (total IgG concentrations in samples: IgG_{CON} 20 mg/mL, IgG_{AQP4} 20 mg/mL, anti-mouse IgG_{MOG} 4.74 mg/mL) and 2 μL hC and sacrificed the mice 5 days post-treatment. Immunofluorescence staining revealed human IgG-positive areas in all three groups, while only the IgG_{AQP4}/IgG_{MOG} plus hC groups showed C5b-9 deposition (Fig. 4A), suggesting the activation of exogenous complement.

Compared with the control group (IgG_{CON} plus hC), intracerebral injection of IgG_{AQP4} and hC caused a marked loss of AQP4 ($P < 0.0001$), GFAP ($P = 0.0005$), and MBP ($P = 0.0119$) (Fig. 4B). In comparison with IgG_{CON}, IgG_{MOG} and hC mainly produced extensive demyelination with loss of MBP ($P = 0.0119$), as well as loss of GFAP ($P = 0.0470$) and AQP4 ($P = 0.0053$) (Fig. 4B). Thus, injection of IgG_{MOG} plus hC also damaged astrocytes in mice. To show the differences between IgG_{AQP4} and IgG_{MOG} lesions more directly, the ratios of AQP4-depleted areas to MBP-depleted areas (S_{AQP4}/S_{MBP}) were compared between the two groups. We found that S_{AQP4}/S_{MBP} was > 1 in the IgG_{AQP4} plus hC group, while S_{AQP4}/S_{MBP} was < 1 in the IgG_{MOG} plus hC group ($P = 0.0079$) (Fig. 4C). These results showed that IgG_{AQP4} mainly causes marked damage to astrocytes, while IgG_{MOG} causes demyelination.

Immunostaining revealed extensive inflammatory infiltrates that included macrophages, neutrophils, and $CD3^+$ T cells in the brains of mice that received IgG_{AQP4} or IgG_{MOG} with hC (Fig. 5A, B). Compared with those that received IgG_{CON}, mice receiving IgG_{AQP4} in the presence of hC had increased numbers of macrophages and neutrophils (both: $P = 0.0079$) and a non-significant trend toward increased $CD3^+$ T cells ($P = 0.0556$) (Fig. 5C). Similarly, treatment with IgG_{MOG} plus hC caused infiltration of macrophages and neutrophils (both: $P = 0.0079$) but not $CD3^+$ T cells ($P = 0.0317$) (Fig. 5C).

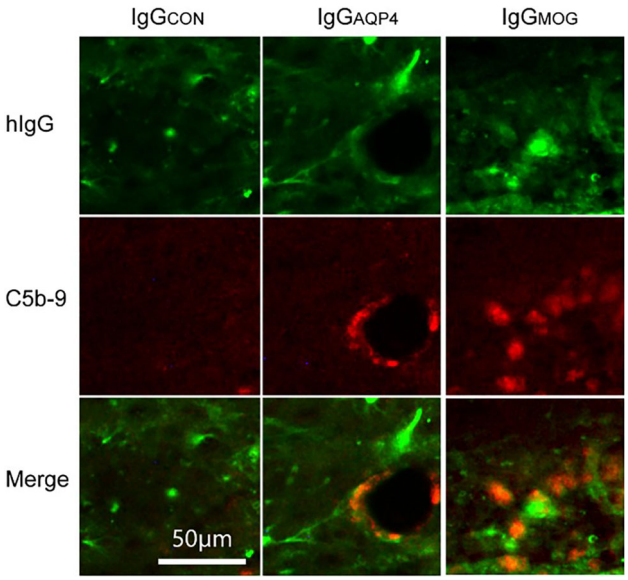

Fig. 6 IgG_{AQP4} and IgG_{MOG} successfully activated the rat complement system. Rats receiving 10 μL total IgG (IgG_{CON}, IgG_{AQP4}, or IgG_{MOG}) without hC were killed at 5 days and brain sections immunostained with human IgG (hIgG) and C5b-9. Human IgG-positive areas (green) were seen in all three groups, while only IgG_{AQP4}/IgG_{MOG} caused C5b-9 deposition (red).

IgG_{AQP4} and IgG_{MOG} Caused Lesions in Rat Brain *Via* Complement Activation

Collecting sufficient IgG_{MOG} for rat studies was challenging because of the rarity of patients whose MOG-IgG cross-reacts with rat MOG. Thus, the three rats in each group were sufficient for data description but not for statistical analyses. Rats have an active complement system similar to humans [35], so we injected 10 μL of total IgG (IgG_{AQP4}, IgG_{MOG}, or IgG_{CON}) into rat brains without hC [36] to induce lesions. Five days post-treatment, human IgG binding was observed in all three groups

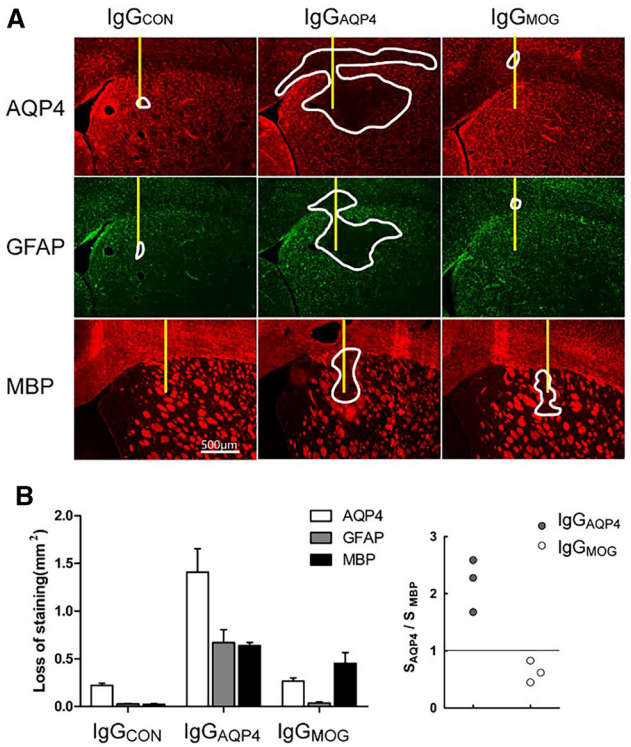

Fig. 7 Pathology in rat brains injected with IgG_{AQP4} and IgG_{MOG}. Rats receiving 10 μL total IgG (IgG_{CON}, IgG_{AQP4}, or IgG_{MOG}) without hC were killed at 5 days and immunostained for AQP4, GFAP, and MBP. **A** Representative images (yellow lines, needle tracks; white lines, lesion borders). **B** Left, areas of loss of AQP4, GFAP, and MBP at day 5 (mean ± SEM, $n = 3$). Right, ratios of AQP4- to MBP-depleted areas (S_{AQP4}/S_{MBP}) in the two groups ($n = 3$).

and C5b-9-positive immunostaining was evident only in the two experimental groups (rats receiving IgG_{AQP4} or IgG_{MOG}) (Fig. 6), indicating that IgG_{AQP4} and IgG_{MOG} successfully activate the rat complement system.

NMOSD-like lesions developed in rats 5 days after intracerebral injection of IgG_{AQP4}, with marked loss of AQP4 and GFAP and mild loss of MBP around the needle track (Fig. 7A, B). In comparison, IgG_{MOG} caused mild loss of MBP in rats but no loss of astrocytes, as shown by immunostaining for AQP4 and GFAP (Fig. 7A, B). Lesions did not occur in rats injected with IgG_{CON}. To further confirm the finding that AQP4-IgG mainly causes astrocyte damage while MOG-IgG mainly targets myelin, the S_{AQP4}/S_{MBP} ratios were compared between rats receiving IgG_{AQP4} and IgG_{MOG}. As shown in Fig. 7B, S_{AQP4}/S_{MBP} was > 1 in the IgG_{AQP4} group while it was < 1 in the IgG_{MOG} group, similar to the data from mice.

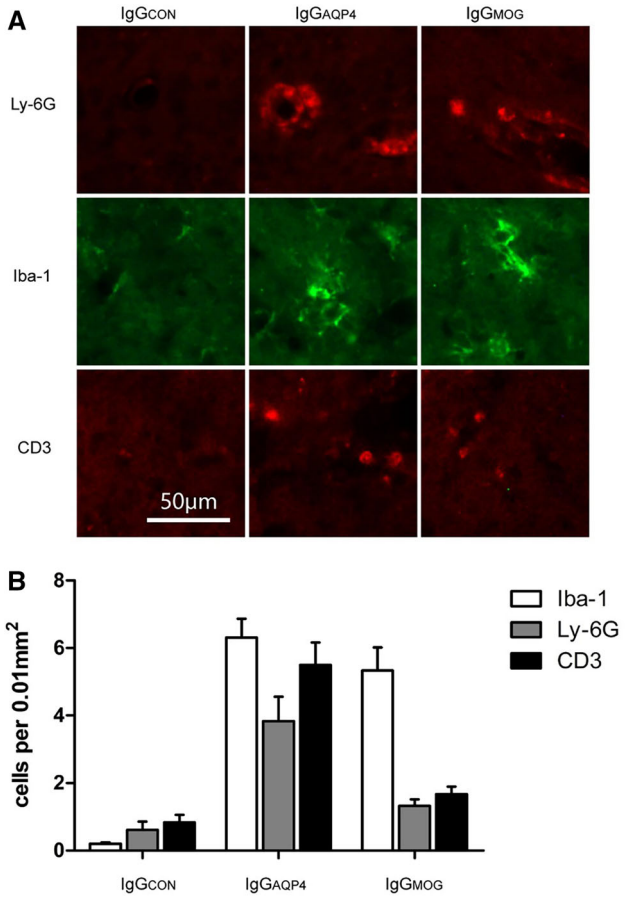

Fig. 8 Inflammatory cell infiltration in rats receiving IgG_{AQP4} or IgG_{MOG}. Rats administered 10 μL total IgG (IgG_{CON}, IgG_{AQP4} or IgG_{MOG}) without hC were killed at 5 days and brain sections stained for immunofluorescence. **A** Representative images of Ly-6G (neutrophils), Iba-1 (macrophages/microglia), and CD3 (T lymphocytes) immunofluorescence. **B** Summary of the numbers of infiltrating cells per 0.01 mm^2 (mean ± SEM, $n = 3$).

Representative images of the immunofluorescence of the inflammatory cell markers Ly-6G (neutrophils), Iba-1 (macrophages/microglia), and CD3 (T cells) are shown in Fig. 8A. IgG_{AQP4} caused marked infiltration of inflammatory cells that were primarily macrophages/microglia but also included some neutrophils and $CD3^+$ cells. IgG_{MOG} led to the infiltration of microglia/macrophages, but few neutrophils and $CD3^+$ cells were present. Rats that received IgG_{CON} were negative for all of these markers (Fig. 8B).

Distinct Ultrastructural Changes Induced by IgG_{AQP4} and IgG_{MOG} in Mouse Brain

To further investigate the pathogenicity of IgG_{AQP4} and IgG_{MOG} in the presence of hC, we investigated the ultrastructure of mouse brain lesions using electron microscopy. Severe swelling of astrocyte end-feet was observed in mice that received IgG_{AQP4} plus hC; few organelles and loss of cytoskeleton were seen in the end-feet (Fig. 9). However, IgG_{MOG} caused only slight swelling of end-feet in the presence of hC and resulted in mild organelle and cytoskeletal loss (Fig. 9). IgG_{CON} caused mild edema in astrocyte end-feet and no ultrastructural damage was apparent (Fig. 9).

Myelin and oligodendrocytes were normal in mice administered IgG_{CON} and hC (Fig. 10A). Treatment with IgG_{AQP4} plus hC caused damage to myelin (Fig. 10B), including splitting (Fig. 10C 2,3) and loosening (Fig. 10C 3,5) of myelin layers, discontinuity of myelin sheaths, and complete demyelination (Fig. 10B, C 1,4) with axon injury (Fig. 10B, C 1,4). Injection of IgG_{MOG} plus hC induced patchy demyelination (Fig. 10D 1,2), abnormal axon morphology with thinner myelin sheaths (Fig. 10D 4), and scattered fragmentation of myelin (Fig. 10D 2,3,5) along with phagocytes engulfing and destroying the debris from damaged tissue (Fig. 10D 1). IgG_{MOG} also caused clear organelle edema in oligodendrocytes (Fig. 11A). In addition, there were nuclear vacuoles in neurons in the group given IgG_{AQP4} plus hC (Fig. 11B).

Discussion

This study is of interest because of our findings that (i) MOG-IgG only caused demyelination in the presence of complement; (ii) MOG-IgG induced astrocyte damage in mouse brain; and (iii) ultrastructural changes induced by AQP4-IgG and MOG-IgG included edema of astrocyte end-feet, organelle edema in oligodendrocytes, and the appearance of nuclear vacuoles in neurons.

We confirmed that, in the absence of complement, MOG-IgG does not induce damage to cells and

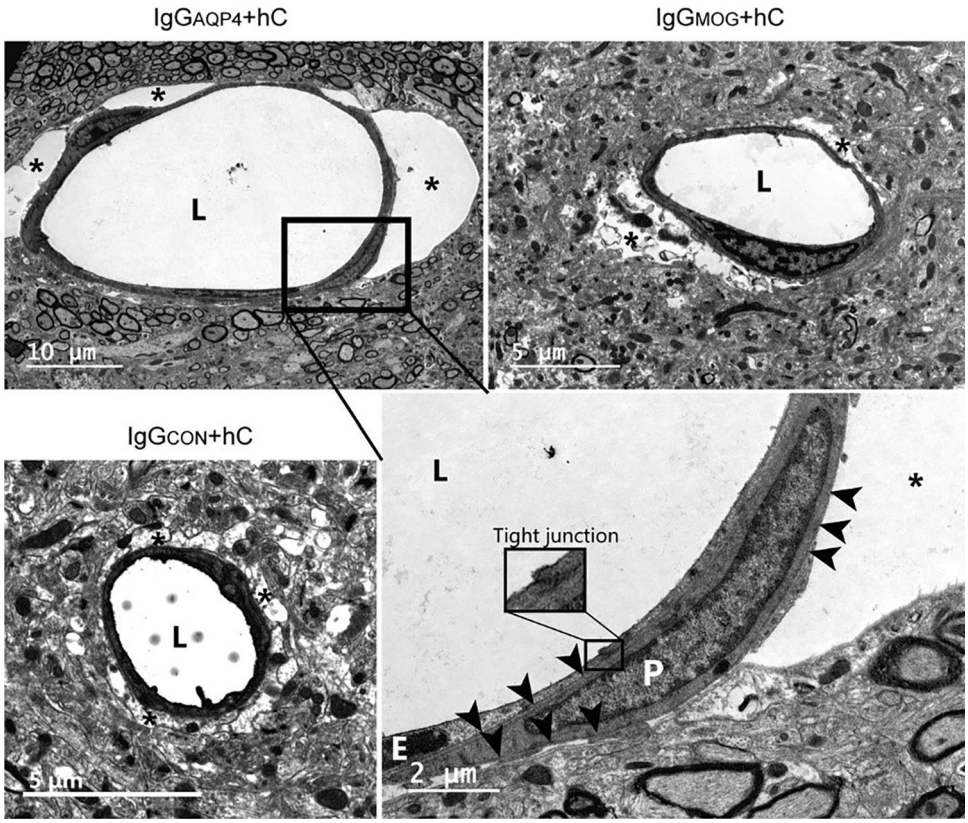

Fig. 9 Representative electron microscopic images of the blood-brain barrier 10 days after intracerebral injection of 3 μL total IgG (IgG_{CON}, IgG_{AQP4}, or IgG_{MOG}) plus 2 μL hC into mouse brain. L, lumen of blood vessel; P, pericyte; E, endothelial cell; arrowheads, basement membrane; asterisks, end-feet of astrocytes.

inflammatory infiltration in lesions. These results tallied with those of previous studies. One previous study showed that antibodies to MOG and AQP4 in patients are predominantly of the IgG1 subtype and mediate complement-dependent cytotoxicity at high titers [31]. Patrick *et al.* showed that purified IgG from one patient with high titers of anti-human, -mouse, and -rat MOG antibodies and robust binding to myelin tissue elicited significant complement-mediated myelin loss in organotypic brain slices, but not in a mouse model of experimental autoimmune encephalomyelitis [29]. A recent study revealed that MOG-specific antibodies affinity-purified from patients with inflammatory demyelinating disease induce pathological changes *in vivo* upon co-transfer with myelin-reactive T cells; when MOG-specific antibodies are co-transferred with MBP-specific T cells, they induce demyelination associated with the deposition of C5b-9, resembling the pathology of multiple sclerosis type II [33]. Interestingly, other studies have suggested that lesions in the mouse brain caused by human MOG-IgG are not associated with inflammatory cell infiltration and occur largely independent of complement [28, 32]. Human MOG-IgG induces the death of MOG-expressing target cells *in vitro* (complement activity in anti-MOG antibody-negative and -positive sera did not differ significantly in the experiments), and enhance demyelination and axonal damage when transferred to animals with autoimmune encephalomyelitis [32]. In addition, these changes recovered within two weeks and no astrocyte damage occurred [28]. Moreover, human MOG-IgG also harms the cytoskeletal structure of oligodendrocytes [37]. MOG-IgG belongs mainly to the IgG1 subclass, but IgG2, IgG3, and IgG4 antibodies are also detectable [38]. The manner in which different IgG subclasses damage target cells may contribute to the different results of previous studies.

To date, there have been no reports of human MOG-IgG inducing astrocyte damage. Our study showed that human MOG-IgG induced not only loss of myelin, but also organelle edema in oligodendrocytes and astrocyte death in mouse brain lesions. The mechanism of damage to astrocytes is not clear, but may be secondary to the damage to oligodendrocytes and the formation of an inflammatory microenvironment containing cytokines, inflammatory cells, and microRNAs [39, 40]. Whether human MOG-IgG damages astrocytes *via* a complement bystander mechanism, which may explain the early oligodendrocyte injury and demyelination in AQP4-IgG-positive NMOSD patients [41], remains to be verified.

Compared with lesions in mouse brains, the range of lesion sizes in rat brains was smaller and no astrocyte injury was observed. These discrepancies may be due to the low effective concentration of MOG-IgG and complement

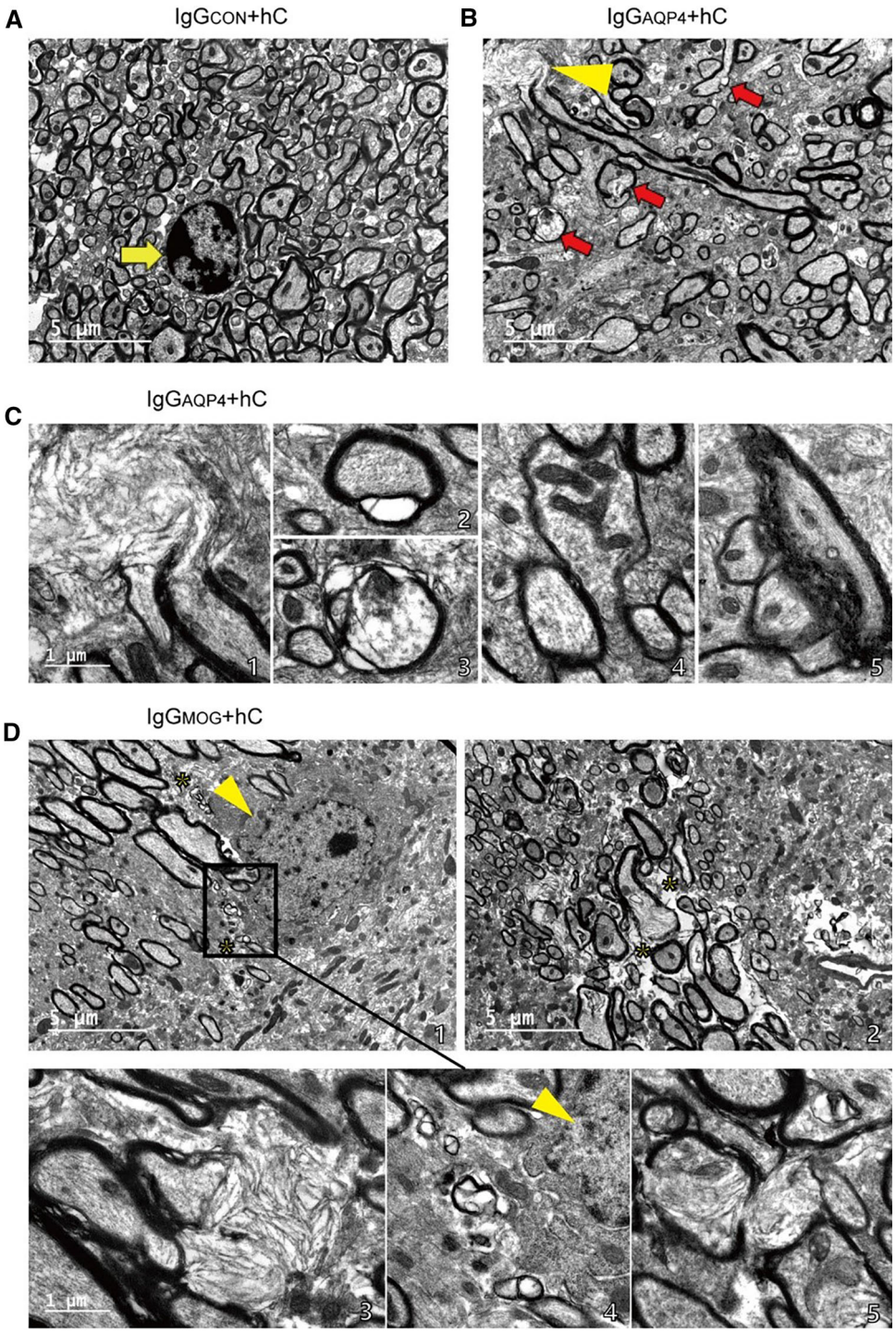

Fig. 10 Ultrastructural changes of myelin sheaths and axons 10 days after intracerebral injection of 3 μL total IgG (IgG_{CON}, IgG_{AQP4}, or IgG_{MOG}) plus 2 μL human complement into mouse brain. **A** Normal oligodendrocyte in a mouse from the IgG_{CON} plus hC group (arrow) with normal surrounding myelin. **B** Image from an IgGAQP4 + hC mouse (yellow arrowhead, entire demyelination at an axonal terminal; red arrow, scattered damage to myelin). **C** Images from IgG_{AQP4} + hC mice. 1, axonal terminal in **B** under higher power; 2–5, demyelination. **D** Myelin sheath injury in the IgG_{MOG} plus hC group. 1, 2. *Patchy loss of myelin; yellow arrowhead, phagocyte; 3–5, demyelination (arrowhead in 4, phagocyte).

activation across species. Whether human MOG-IgG can directly or indirectly cause damage to astrocytes in rats is still uncertain, although no loss of AQP4 and GFAP was found by immunofluorescence. Limited by the shortage of high levels of MOG-IgG in patients, we could not further verify the pathogenic effects of human MOG-IgG on rat MOG.

The different pathogenic mechanisms of AQP4-IgG and MOG-IgG were clearly apparent (Table 2). In our study, both AQP4-IgG and MOG-IgG induced damage to astrocytes and myelin in mice, followed by the infiltration of inflammatory cells dependent on complement activation. AQP4-IgG mainly caused astrocyte injury and secondary demyelination, while MOG-IgG targeted the myelin sheath directly and induced astrocyte damage in mice. By electron

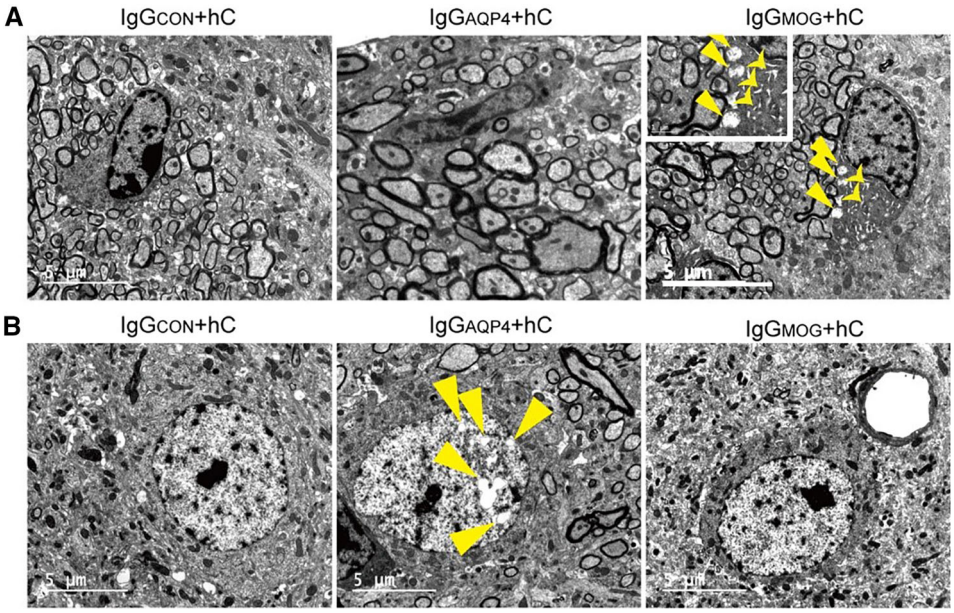

Fig. 11 Ultrastructural changes in oligodendrocytes and neurons 10 days after intracerebral injection of 3 μl total IgG (IgG_{CON}, IgG_{AQP4}, or IgG_{MOG}) plus 2 μL hC into mouse brain. **A** Oligodendrocytes were normal in mice with IgG_{CON} (left) and IgG_{AQP4} (middle) in the presence of hC. IgG_{MOG} plus hC (right) caused marked organelle edema in oligodendrocyte (long arrowheads, mitochondrial swelling; short arrowheads, smooth endoplasmic reticulum extension). **B** Neurons from mice with IgG_{CON} (left) and IgG_{MOG} (right) in the presence of hC were normal. IgG_{AQP4} plus hC induced nuclear vesicles in neurons (middle; long arrowheads, nuclear vesicles).

Table 2 Comparison of lesions induced by AQP4-IgG and MOG-IgG in rodent brains.

	AQP4-IgG	MOG-IgG
Target cell	Astrocyte (AQP4 expressed on end-foot surface)	Oligodendrocyte (MOG expressed on myelin sheath)
Complement activation	Yes	Yes
	Complement deposition	Complement deposition
Endogenous complement activation	Yes (rat)/No (mouse)	Yes (rat)/No (mouse)
Astrocyte		
Loss of AQP4	Yes, major	Yes, minor (mouse)/No (rat)
Loss of GFAP	Yes, marked but less than AQP4	Yes, minor (mouse)/No (rat)
Ultrastructure	Marked edema and loss of cytoplasm structure of end-feet	Mild edema and part of cytoplasm structure of end-feet missing
Oligodendrocyte		
Loss of MBP	Yes, marked but less than AQP4	Yes, marked and more than APQ4
Ultrastructure	Demyelination	Patchy demyelination; destruction of oligodendrocyte cytoskeleton [35], mitochondrial swelling and smooth endoplasmic reticulum extension
Neuron		
Ultrastructure	Nuclear vesicles, axonal injury	Axonal injury
Inflammatory infiltration	Yes	Yes

microscopy, marked edema of astrocytes was apparent in mice treated with IgG_{AQP4} and hC, especially in end-feet, as well as demyelination, nuclear vesicle formation in neurons, and axon injury In comparison, MOG-IgG caused more severe and patchy loss of myelin with damage to oligodendrocyte organelles, but mild swelling of astrocyte end-feet. Marie-Theres *et al*. found that myelin breakdown appears to begin at the inner layers and progressed outward

over time after injecting AQP4-IgG (rAB-53) into mouse brains, while the fragmentation patterns induced by anti-MOG antibodies (8-18C5) are more heterogeneous [42].

Our study had several limitations. First, the low concentration of MOG-IgG and other constituents in total patient IgG may have led to uncertainty in our results. Second, we need to obtain more human MOG-IgG with cross-reactivity against rat MOG for further investigations of its pathogenicity in rats. One possible approach to resolve these problems is to screen for B-cells secreting MOG-IgG and produce monoclonal antibodies against MOG for future research.

In conclusion, human MOG-IgG led to cell death by activating hC *in vitro* and *in vivo*. While AQP4-IgG directly targeted astrocytes, MOG-IgG mainly damaged oligodendrocytes.

Acknowledgements This work was supported by grants from the National Natural Science Foundation of China (81471218 and 81771300) and the Natural Science Foundation of Guangdong Province, China (2017A030313853). We thank Professors Yiwen Ruan and Yunfeng Shi at Jinan University who supported the electron microscopy experiments.

Conflict of Interest The authors declare that they have no conflict of interest.

References

1. Lennon VA, Wingerchuk DM, Kryzer TJ, Pittock SJ, Lucchinetti CF, Fujihara K, *et al*. A serum autoantibody marker of neuromyelitis optica: distinction from multiple sclerosis. Lancet 2004, 364: 2106–2112.
2. Parratt JD, Prineas JW. Neuromyelitis optica: a demyelinating disease characterized by acute destruction and regeneration of perivascular astrocytes. Mult Scler 2010, 16: 1156–1172.
3. Wingerchuk DM, Banwell B, Bennett JL, Cabre P, Carroll W, Chitnis T, *et al*. International consensus diagnostic criteria for neuromyelitis optica spectrum disorders. Neurology 2015, 85: 177–189.
4. Sato DK, Callegaro D, Lana-Peixoto MA, Waters PJ, de Haidar JF, Takahashi T, *et al*. Distinction between MOG antibody-positive and AQP4 antibody-positive NMO spectrum disorders. Neurology 2014, 82: 474–481.
5. Hamid S, Whittam D, Mutch K, Linaker S, Solomon T, Das K, *et al*. What proportion of AQP4-IgG-negative NMO spectrum disorder patients are MOG-IgG positive? A cross sectional study of 132 patients. J Neurol 2017, 264: 2088–2094.
6. O'Connor KC, McLaughlin KA, De Jager PL, Chitnis T, Bettelli E, Xu C, *et al*. Self-antigen tetramers discriminate between myelin autoantibodies to native or denatured protein. Nat Med 2007, 13: 211–217.
7. Waters P, Reindl M, Saiz A, Schanda K, Tuller F, Kral V, *et al*. Multicentre comparison of a diagnostic assay: aquaporin-4 antibodies in neuromyelitis optica. J Neurol Neurosurg Psychiatry 2016, 87: 1005–1015.
8. Sepulveda M, Armangue T, Martinez-Hernandez E, Arrambide G, Sola-Valls N, Sabater L, *et al*. Clinical spectrum associated with MOG autoimmunity in adults: significance of sharing rodent MOG epitopes. J Neurol 2016, 263: 1349–1360.
9. Jarius S, Ruprecht K, Kleiter I, Borisow N, Asgari N, Pitarokoili K, *et al*. MOG-IgG in NMO and related disorders: a multicenter study of 50 patients. Part 2: Epidemiology, clinical presentation, radiological and laboratory features, treatment responses, and long-term outcome. J Neuroinflammation 2016, 13: 280.
10. Yan Y, Li Y, Fu Y, Yang L, Su L, Shi K, *et al*. Autoantibody to MOG suggests two distinct clinical subtypes of NMOSD. Sci China Life Sci 2016, 59: 1270–1281.
11. Haase CG, Guggenmos J, Brehm U, Andersson M, Olsson T, Reindl M, *et al*. The fine specificity of the myelin oligodendrocyte glycoprotein autoantibody response in patients with multiple sclerosis and normal healthy controls. J Neuroimmunol 2001, 114: 220–225.
12. von Budingen HC, Hauser SL, Fuhrmann A, Nabavi CB, Lee JI, Genain CP. Molecular characterization of antibody specificities against myelin/oligodendrocyte glycoprotein in autoimmune demyelination. Proc Natl Acad Sci U S A 2002, 99: 8207–8212.
13. Breithaupt C, Schubart A, Zander H, Skerra A, Huber R, Linington C, *et al*. Structural insights into the antigenicity of myelin oligodendrocyte glycoprotein. Proc Natl Acad Sci U S A 2003, 100: 9446–9451.
14. von Budingen HC, Hauser SL, Ouallet JC, Tanuma N, Menge T, Genain CP. Frontline: Epitope recognition on the myelin/oligodendrocyte glycoprotein differentially influences disease phenotype and antibody effector functions in autoimmune demyelination. Eur J Immunol 2004, 34: 2072–2083.
15. Brehm U, Piddlesden SJ, Gardinier MV, Linington C. Epitope specificity of demyelinating monoclonal autoantibodies directed against the human myelin oligodendrocyte glycoprotein (MOG). J Neuroimmunol 1999, 97: 9–15.
16. Kitley J, Waters P, Woodhall M, Leite MI, Murchison A, George J, *et al*. Neuromyelitis optica spectrum disorders with aquaporin-4 and myelin-oligodendrocyte glycoprotein antibodies: a comparative study. JAMA Neurol 2014, 71: 276–283.
17. Hyun JW, Woodhall MR, Kim SH, Jeong IH, Kong B, Kim G, *et al*. Longitudinal analysis of myelin oligodendrocyte glycoprotein antibodies in CNS inflammatory diseases. J Neurol Neurosurg Psychiatry 2017, 88: 811–817.
18. Stiebel-Kalish H, Lotan I, Brody J, Chodick G, Bialer O, Marignier R, *et al*. Retinal nerve fiber layer may be better preserved in MOG-IgG versus AQP4-IgG optic neuritis: a cohort study. PLoS One 2017, 12: e170847.
19. Pandit L, Nakashima I, Mustafa S, Takahashi T, Kaneko K. Anti Myelin Oligodendrocyte Glycoprotein associated Immunoglobulin G (AntiMOG-IgG)-associated neuromyelitis optica spectrum disorder with persistent disease activity and residual cognitive impairment. Ann Indian Acad Neurol 2017, 20: 411–413.
20. Hamid S, Whittam D, Saviour M, Alorainy A, Mutch K, Linaker S, *et al*. Seizures and encephalitis in myelin oligodendrocyte glycoprotein IgG disease vs aquaporin 4 IgG disease. JAMA Neurol 2018, 75: 65–71.
21. Zhou Y, Jia X, Yang H, Chen C, Sun X, Peng L, *et al*. Myelin oligodendrocyte glycoprotein (MOG) antibody-associated demyelination: comparison between onset phenotypes. Eur J Neurol 2018,26:175–183.
22. Chen L, Chen C, Zhong X, Sun X, Zhu H, Li X, *et al*. Different features between pediatric-onset and adult-onset patients who are seropositive for MOG-IgG: A multicenter study in South China. J Neuroimmunol 2018, 321: 83–91.
23. Kinoshita M, Nakatsuji Y, Kimura T, Moriya M, Takata K, Okuno T, *et al*. Neuromyelitis optica: passive transfer to rats by human immunoglobulin. Biochem Biophys Res Commun 2009, 386: 623–627.
24. Linington C, Bradl M, Lassmann H, Brunner C, Vass K. Augmentation of demyelination in rat acute allergic encephalomyelitis by circulating mouse monoclonal antibodies

directed against a myelin/oligodendrocyte glycoprotein. Am J Pathol 1988, 130: 443–454.
25. Piddlesden SJ, Lassmann H, Zimprich F, Morgan BP, Linington C. The demyelinating potential of antibodies to myelin oligodendrocyte glycoprotein is related to their ability to fix complement. Am J Pathol 1993, 143: 555–564.
26. Mayer MC, Breithaupt C, Reindl M, Schanda K, Rostasy K, Berger T, *et al*. Distinction and temporal stability of conformational epitopes on myelin oligodendrocyte glycoprotein recognized by patients with different inflammatory central nervous system diseases. J Immunol 2013, 191: 3594–3604.
27. Marta CB, Oliver AR, Sweet RA, Pfeiffer SE, Ruddle NH. Pathogenic myelin oligodendrocyte glycoprotein antibodies recognize glycosylated epitopes and perturb oligodendrocyte physiology. Proc Natl Acad Sci U S A 2005, 102: 13992–13997.
28. Saadoun S, Waters P, Owens GP, Bennett JL, Vincent A, Papadopoulos MC. Neuromyelitis optica MOG-IgG causes reversible lesions in mouse brain. Acta Neuropathol Commun 2014, 2: 35.
29. Peschl P, Schanda K, Zeka B, Given K, Bohm D, Ruprecht K, *et al*. Human antibodies against the myelin oligodendrocyte glycoprotein can cause complement-dependent demyelination. J Neuroinflammation 2017, 14: 208.
30. Weinshenker BG, Wingerchuk DM. Neuromyelitis spectrum disorders. Mayo Clin Proc 2017, 92: 663–679.
31. Mader S, Gredler V, Schanda K, Rostasy K, Dujmovic I, Pfaller K, *et al*. Complement activating antibodies to myelin oligodendrocyte glycoprotein in neuromyelitis optica and related disorders. J Neuroinflammation 2011, 8: 184.
32. Zhou D, Srivastava R, Nessler S, Grummel V, Sommer N, Bruck W, *et al*. Identification of a pathogenic antibody response to native myelin oligodendrocyte glycoprotein in multiple sclerosis. Proc Natl Acad Sci U S A 2006, 103: 19057–19062.
33. Spadaro M, Winklmeier S, Beltran E, Macrini C, Hoftberger R, Schuh E, *et al*. Pathogenicity of human antibodies against myelin oligodendrocyte glycoprotein. Ann Neurol 2018, 84: 315–328.
34. Ratelade J, Verkman AS. Inhibitor(s) of the classical complement pathway in mouse serum limit the utility of mice as experimental models of neuromyelitis optica. Mol Immunol 2014, 62: 104–113.
35. Asavapanumas N, Ratelade J, Verkman AS. Unique neuromyelitis optica pathology produced in naive rats by intracerebral administration of NMO-IgG. Acta Neuropathol 2014, 127: 539–551.
36. Asavapanumas N, Verkman AS. Neuromyelitis optica pathology in rats following intraperitoneal injection of NMO-IgG and intracerebral needle injury. Acta Neuropathol Commun 2014, 2: 48.
37. Dale RC, Tantsis EM, Merheb V, Kumaran RY, Sinmaz N, Pathmanandavel K, *et al*. Antibodies to MOG have a demyelination phenotype and affect oligodendrocyte cytoskeleton. Neurol Neuroimmunol Neuroinflamm 2014, 1: e12.
38. Mariotto S, Ferrari S, Monaco S, Benedetti MD, Schanda K, Alberti D, *et al*. Clinical spectrum and IgG subclass analysis of anti-myelin oligodendrocyte glycoprotein antibody-associated syndromes: a multicenter study. J Neurol 2017, 264: 2420–2430.
39. Fang X, Sun D, Wang Z, Yu Z, Liu W, Pu Y, *et al*. MiR-30a positively regulates the inflammatory response of microglia in experimental autoimmune encephalomyelitis. Neurosci Bull 2017, 33: 603–615.
40. Li AL, Zhang JD, Xie W, Strong JA, Zhang JM. Inflammatory changes in paravertebral sympathetic ganglia in two rat pain models. Neurosci Bull 2018, 34: 85–97.
41. Tradtrantip L, Yao X, Su T, Smith AJ, Verkman AS. Bystander mechanism for complement-initiated early oligodendrocyte injury in neuromyelitis optica. Acta Neuropathol 2017, 134: 35–44.
42. Weil M, Mobius W, Winkler A, Ruhwedel T, Wrzos C, Romanelli E, *et al*. Loss of myelin basic protein function triggers myelin breakdown in models of demyelinating diseases. Cell Reports 2016, 16: 314–322.